Data Quality control procedures and monitoring results in the Japan Meteorological Agency

K. Kashiwagi and A. Baba

Numerical Prediction Division
Japan Meteorological Agency
Tokyo, 100, Japan

1. INTRODUCTION

Three kinds of objective analyses are performed in JMA. One is a global analysis and others are regional analyses for the limited area models. Specifications of the systems are summarized in Table 1. Because the erroneous data extremely degrade the quality of analysis, the quality control of data is a vital component of the analysis systems. This paper describes the real-time quality control procedures applied in the different stages of the JMA analysis systems.

We also perform the non-real-time monitoring of data quality. We find serious systematic errors in the results of our monitoring. Most of them had already been presented in the report of ECMWF/WMO workshop on radiosonde data quality and monitoring held in December 1987. However, our results indicate that they have been hardly amended until now. Therefore, we show some examples of our monitoring and discuss the importance of these problems.

2. QUALITY CONTROL PROCEDURES

Fig.1 illustrates the major functional components and data flow in our 6-hourly intermittent global data assimilation system. In the following, we describe the control procedures applied in the different stages of the system.

2.1 Automatic data processing stage

Observational data received from the GTS and the domestic communication lines are decoded according to their code forms. Bogus data prepared from manual analysis are manually inputted by the operator, if necessary. The most important purpose of bogus data is to incorporate typhoons over the oceans into the objective analysis. On rare occasions they are also used in the global analysis in order to correct the erroneous data which are not rejected in the regional analysis.

All the messages are checked against the WMO international code forms. If code form errors are found, some automatic processes are carried out to recover the apparent errors and to extract the maximum information. In the case of TEMP Part-A, the flags of code form errors are recorded on the decoded data.

Same observations are frequently reported from different communication lines. These duplicate reports are removed or edited according to the reception times, the incoming communication lines and contents of reports.

After these processes, the decoded data are sorted according to their observation types and geographical locations and stored in a file on magnetic disk.

In order to check the availability of data, the number of received bulletins and sorted reports are displayed on the console. If operators find any abnormal state, more detailed information and data coverage maps can be quickly printed out.

2.2 Pre-analysis stage

Data to be used in the analysis are extracted from the sorted data file.

A check of climatological reasonability is performed for all the types of data. A check of vertical consistency is performed for TEMP and PILOT data using Part-A,B,C,D and SYNOP data. The items of the check are listed below:

(1) Icing of instrument
(2) Consistency between sonde data at the lowest level and surface data
(3) Consistency between the data at standard levels and the data at significant levels
(4) Temperature lapse rate
(5) Hydrostatic relationship
(6) Vertical wind shear

A lapse rate check for SATEM is also performed using the mean virtual temperature calculated from the thickness.

Furthermore, solar radiation corrections are made for TEMP data above 150hPa level using a simple statistical correction of the day soundings to the night soundings. The factors considered in the statistics are pressure level, solar angle, type of instrument and country.

After these checks, data are merged and re-arranged according to the analysis grid systems for the convenience of analysis and stored on a magnetic disk together with information of vertical check.

2.3 Analysis stage

A gross error check and horizontal consistency check are performed in order to remove erroneous or unrepresentative observations in advance of analysis.

The observation-minus-guess residual (D) is calculated for every observation. The residuals are compared with two types of tolerance limits C_1 and C_2 which are based on the forecast error standard deviations. If $D \gtrsim C_1$, the data are rejected. If $C_1 > D > C_2$, the data are checked by interpolating neighbouring data to the location of the data. The data which do not agree with the interpolated values within a reasonable tolerance are rejected. A simple two-dimensional uni-variate correction method is used for the interpolation of this check.

After analysis, the information of rejected data and statistics on difference between observation and analysis are stored on the magnetic disk for the purpose of monitoring the quality of observation data and analysed fields. Furthermore, the analysed fields are plotted on maps together with observations. If any abnormal states are detected by operators and/or forecasters from these maps, necessary information is quickly printed out from the disk files.

2.4 Non real-time monitoring

Sorted data, analysed and predicted fields and information on quality control are stored in archival files on optical disk library once a day. We perform the non-real-time monitoring of data quality using these data. Because we use the optimum interpolation method for analysis, the primary purpose of our non-real-time monitoring is to estimate the quality of observations and first-guess. The monitoring is also quite effective to detect suspect stations and systematic errors.

The items of our non-real-time monitoring are listed below:

(1) Compilation of rejected data in real-time monitoring
(2) Calculation of statistics on the difference between observations and first-guess and analysis
(3) Statistical comparison of satellite data with collocated sonde data
(4) Examination of time series of synop and sonde data.

Since 1982, we have been calculating these statistics and developing various computer softwares to display the results in various manners. Some examples and discussion are presented in the next section.

2.5 Future plan

Our real-time quality control procedures work very well in general. However, occasionally, erroneous data are not rejected and correct data are rejected although they could be avoided by human inspection. This is mainly due to the fact that we use the fixed criteria for data rejection regardless of geographical locations and meteorological situations.

In order to improve the performance of our procedures, we are planning to introduce some variable criteria. We also consider the introduction of optimum interpolation method for the horizontal consistency check. Another future plan is to unify the real-time quality control procedures in three analysis stages.

3. MONITORING RESULTS AND DISCUSSION

3.1 Availability of data

The availability of data is the primary factor in a data assimilation system. Fig.2 displays the example for the reception rate of TEMP Part-A during the month of December 1988. The white sectors in the right and left sides of the center lines indicate the reception rate at 00 and 12UTC, respectively. An open circle means that the reception rate is 100%. All stations received at least once during the month are plotted. Our statistical results indicate that the availability is relatively low over Africa, South America and Oceania. The reception rate at night is especially low over these areas.

3.2 Quality of sonde data

Fig.3 shows the ratio of reports with code form errors to all the received reports for TEMP Part-A in December 1988. Fig.4 shows the ratio of reports with rejected data to all the received reports for TEMP and PILOT Part-A in December 1988. It is clear from these figures that the rate of form error and rejection over India are much higher than those over east Asia.

In order to clarify the quality of data furthermore, we show some examples of statistics on the difference between sonde data and first-guess. The rejected data are not included in these statistics.

Fig.5 displays the root mean square geopotential height differences at 500hPa for 00 and 12UTC data in December 1988. Over east Asia, they are very small in general although they vary from region to region. On the other hand, the values over India are twice or three times as large as those over east Asia.

The results are found at other levels and in other variables as well. Instead of showing plane maps, we show the vertical profiles of monthly statistics at station 47936 in Japan and 42339 in India as a typical example. Fig.6 gives standard deviations (right), bias (centre) and root mean square difference (left) of geopotential height (bottom), u-component wind (middle) and v-component wind (top) at these stations. It is clear from this figure that the statistical characteristics over these two regions are quite different.

The numerals between RMS and BIAS in this figure give the number of observations used for calculation. The decrease of the value at upper levels in India might imply that the sondes do not reach higher levels and/or many data at these levels are rejected.

Using these methods, we can detect some areas where the quality of data seems to be much poorer than other areas. We assign larger observation errors for the TEMPs in these areas. However, because these statistical results strongly depend on the quality of first-guess and the method of quality control, the exchange of monitoring results is helpful for the estimation of data quality and performance of the assimilation system.

In this context, the implementation of CBS recommendations on data monitoring and their exchange is quite important. At present, we are participating in the exchange of the results on SHIP data and preparing for submission of all our results in CBS format.

Over the area where the statistical values are relatively homogeneous or gradually vary, we can more easily detect suspect stations.

Fig.7 displays mean geopotential height difference between observation and first-guess at 100hPa for July 1983 00UTC data. We did not perform the solar radiation correction in the analysis system at that time. The most striking feature of the figure is the large uniform positive biases over Japan. However, biases at stations 47580 and 47681 are about 20m lower than those at surrounding stations and the station 47881 shows the large negative bias. We requested the staffs at these stations to examine the data reduction method. Consequently, some errors were found and amended. Furthermore, we were informed that the type of instrument at 47881 differed from others. This example indicates the importance of communication between data producers and users.

We note that these stations are operated by the defence agency and others are operated by JMA. The large biases were mainly caused by a defect of our previous operational prediction model and are greatly reduced in the present model installed in March 1988.

3.3 Solar radiation correction

Fig.7 also shows the large systematic difference of statistical characteristics between different countries. For example, we can find strong discontinuity of bias between 47420 and 32165, 50774 and 31707 and 54292 and 31960. This seems to be mainly caused by difference of instrument and/or solar radiation correction applied at stations. A final solution of this problem must be to use a single type of instrument and data reduction method all over the world. At least the upper-sounding code should be amended to include information on these factors.

Fig.8 displays time series of 100hPa geopotential height in three different areas for December 1988 as a typical example. The solid lines show the variation of reported values and the broken lines denotes the variation of values corrected by our statistical method and vertical consistency check. The circle and asterisk indicate the observations at 00 and 12 UTC, respectively.

The solar radiation correction for Japanese soundings are performed at stations by means of a theoretical method and are not carried out in the analysis system. It is obvious from the time series at 47646 in Japan that the method works very well.

On the other hand, the diagram for 42182 in India shows the remarkably large day-night differences which reach 500m occasionally. Furthermore, the large irregularity with time suggests that the variations include not only effect of solar radiation but also the other factors.

The diagram for 72365 in the United States shows the small but clear day-night difference for some periods. In the periods, our statistical correction method improves the temporal consistency. However, when the reported values do not shows the noticeable day-night difference, the method shows negative effects. This example indicates the limitation of a statistical method at a data processing centre.

The statistics on day-night difference is affected by many factors and it is difficult to separate the effect of solar radiation from others. Furthermore, we can not know changes of instrument and data reduction method in real-time at present. Even if we know these changes, it takes long time and laborious work to estimate reliable statistics. Because data producers know the characteristics of instrument better than users, solar radiation correction should be applied at observation stations as in Japan.

3.4 Effects of a feed back of monitoring results to data producers and automation

Since 1985, we have been giving a lecture on the role of observation in the assimilation system at the training course for operators of sonde soundings once a year. For the lecture, we closely examine the cause of errors comparing our archived informations on rejected data with final sonde data checked by the management division of sonde sounding.

The method of data reduction have already been automated at all stations of JMA. Thus, most of errors were caused by manual operations in encoding and typing. A typical example is failure in following the right order of two adjacent figures. About 20% of these errors were due to the code regulations unsuitable for human operations, that is,

(1) the sign of temperature presented by odd or even number
(2) the inclusion of the units figure of wind direction in the hundreds figure of wind speed
(3) the discontinuity in the units of geopotential height between 700hPa and 500hPa.

The results of our examination are presented in the lecture and submitted to the management division of sonde sounding. Table 2 shows the number of data rejected in our vertical consistency check during the month of April each year. It is clear from the table that the total number of rejected data decreases with year. They are decreased by approximately 60% in four years. Although the reasons are not definite, we believe that the feed back of monitoring results contributes to improvement of data quality to a certain extent.

Since 1986, JMA has been automatizing the encoding and transmission of report in addition to the data reduction. The new procedure was introduced at stations 47646, 47936 and 47412 in 1986, 1987 and 1988, respectively. As shown in Table 2, no data were rejected in the vertical check at these stations after introduction of the new procedure except one case. In the exceptional case, a datum at a significant level was missed in the report. A deficiency which happens under quite rare situations was found in the encoding programme by our indication.

As the automation of observation proceeds, the horizontal consistency check becomes more important. Fig.9 shows another error caused by manual operation. In this case, the operator at station 47918 put the wrong value for the constant of thermistor into the micro-processor. Because there was no other error, the automated procedure guaranteed the vertical consistency and the data were not rejected in the vertical check. However, the geopotential heights above 400hPa were rejected in the horizontal check. For example, at 300hPa level, the reported value was 9850m and the value interpolated at this station from surrounding data was 9727m and the correct value was 9732m.

Above mentioned results clearly demonstrate that automation is quite effective to improve quality of data. However, it should be noted that quality of data still depends on work ethics of operator as far as any manual operations remain in observation and transmission procedures.

3.5 Quality of satellite data

Fig.10 displays an example of statistical comparison between satellite data and collocated sonde data. The solid lines indicate the RMS and mean difference of thickness temperature between sonde data and the collocated SATEMs (within 150km and 6 hours) in various latitude belts for December 1988. The broken lines are the same as solid lines except the difference between sonde data and first-guess interpolated at SATEM observation points.

Because the same sonde data are used for verification of SATEM and first-guess, larger RMS means worse quality. It is clear from this figure that the error of SATEM is larger than those of first guess in the troposphere of middle and high latitudes.

We have the same statistical result for SATOB. Especially, SATOBs at upper levels have large negative biases over middle latitudes in winter.

As numerical prediction models become more sophisticated and their resolutions become higher, it is desired to improve the quality of satellite data as well as their resolution.

4. CONCLUDING REMARKS

The real-time quality control procedures in JMA work very well in general. In order to improve the performance of our procedures, we are planning to introduce the variable criteria and to unify the procedures in three analysis steps.

We find serious problems on data quality in the results of our non-real-time monitoring. We think that the following recommendations are quite effective in order to resolve these problems.

(1) Implementation of CBS recommendations on data monitoring and their exchange
(2) More tightly communication between data producers and users
(3) Automation of data reduction and transmission

We also find systematic difference caused by the difference of instrument and data reduction method. Although a final solution of this problem is to use a single type of instrument all over the world, the upper-sounding code should be amended to include information on these factors at least. Furthermore, solar radiation correction should be applied at observation stations because data producers know the characteristics of instrument better than users.

Table 1 Specification of JMA Operational Objective Analysis

AREA	Global	Asia	Japan
Analysis time	00, 06, 12 18 UTC	00 and 12 UTC	00 and 12 UTC
Cut-off time	6-hours after map time	3.0-hours after map time	3.0-hours after map time
Grid system	Latitude - Longitude	60° Stereographic projection	60° Stereographic projection
Resolution	1.875°	150km at 60°N	80km at 60°N
Number of grid point	192 x 97 (0°E,90°N)=(1,1)	88 x 78 (30°N,140°E)= (56,45)	68 x 68 (30°N,140°E)= (45,46)
Initial guess	6-hours global forecast fields	12-hours global forecast fields	12-hours global forecast fields
Levels	Surface - 10hPa 16 levels	Surface - 100hPa 11 levels	Surface - 100hPa 11 levels
analysed parameters	Mean sea level pressure Surface ------------------------- U, V, T, T-Td 1000hPa ------------------------- Z 850, 700, 500, 400, 300hPa ------- Z, U, V, T, T-Td 250, 200, 150, 100hPa ------------ Z, U, V, T 70, 50, 30, 20, 10hPa ------------ Z,(U, V),T		
Analysis method	Troposphere (Surface - 100hPa) Optimum interpolation method Stratosphere (70hPa - 10hPa) Functional fitting method		
Data used in analysis	SYNOP, SHIP, DRIBU, Australian PAOB, Bogus data, TEMP, PILOT, AIREP, SATEM, SATOB, GMS cloud data		

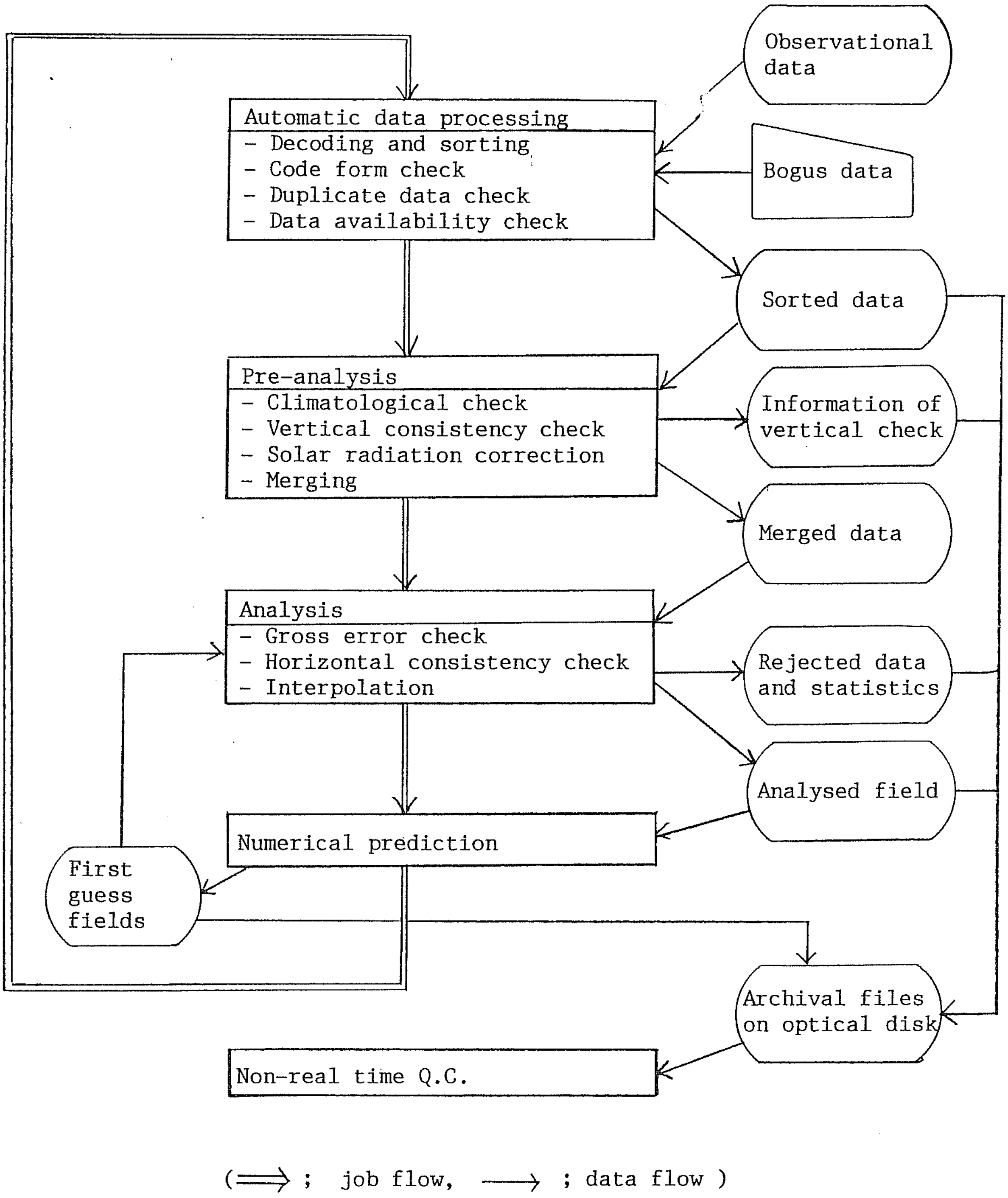

Fig. 1 Major functional components and data flow in the JMA data assimilation system.

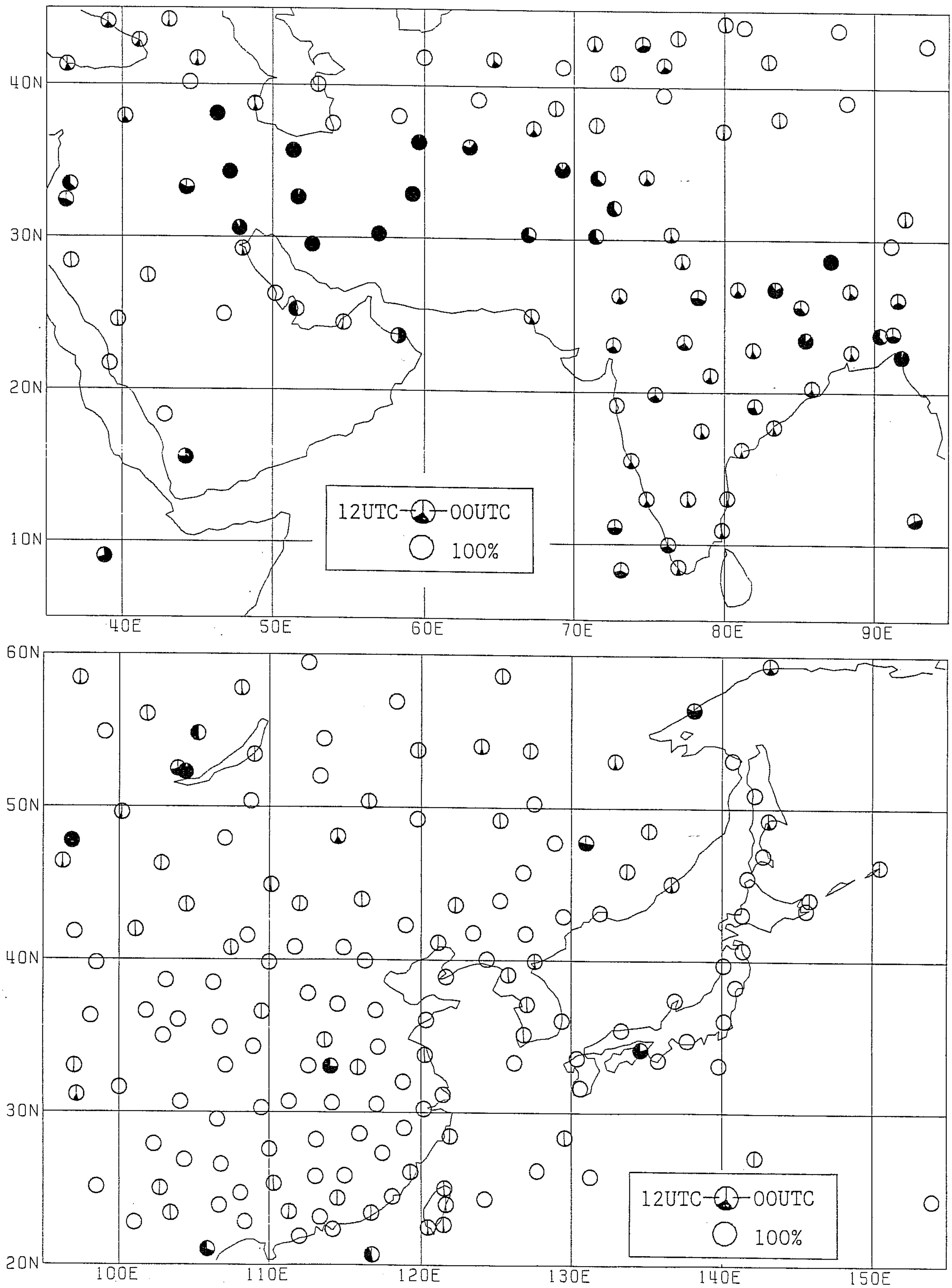

Fig. 2 Reception rate of TEMP Part-A for December 1988.

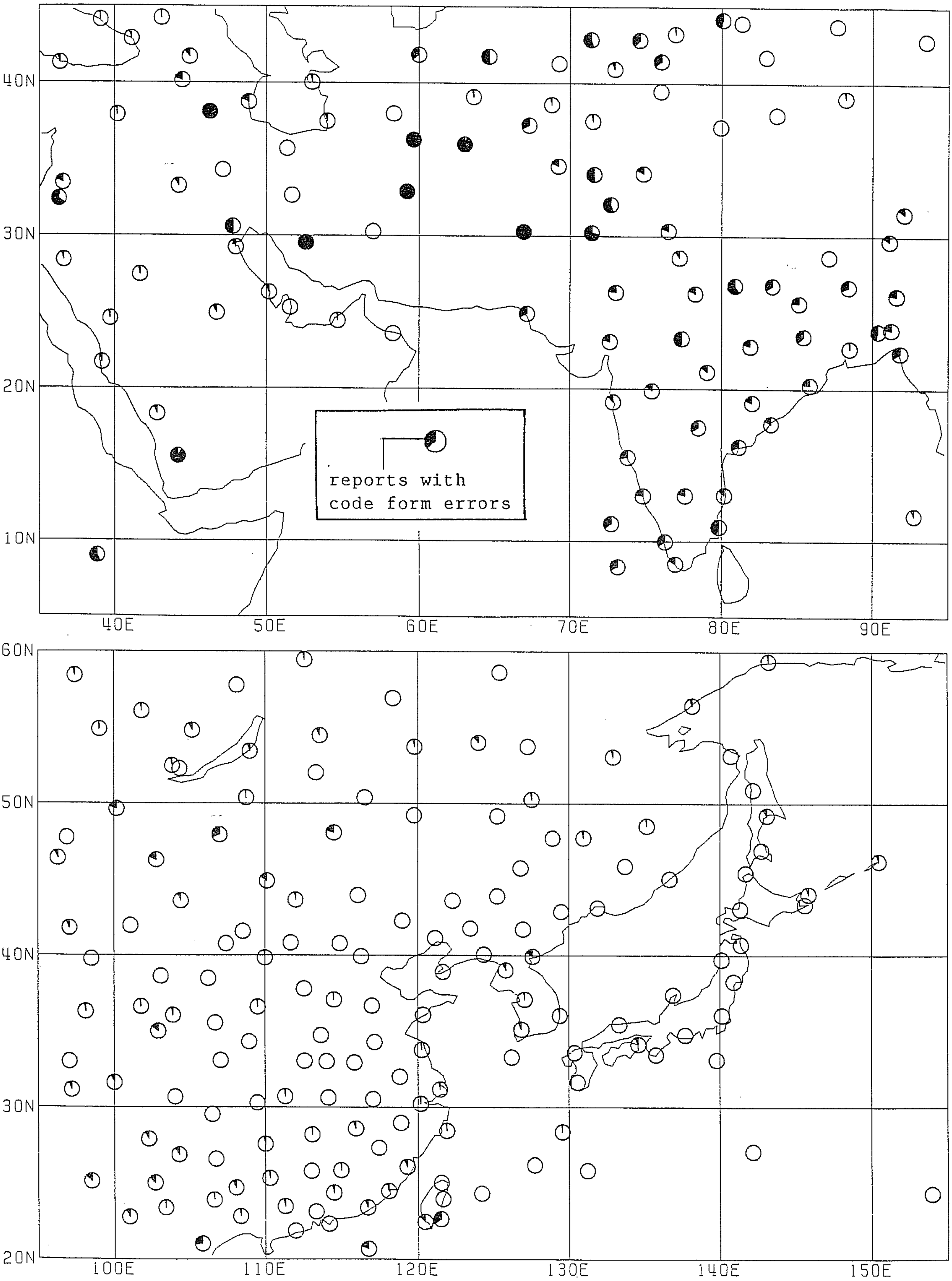

Fig. 3 Ratio of reports with code form errors to all the received reports for TEMP Part-A in December 1988.
Black sector indicates repors with code form errors.

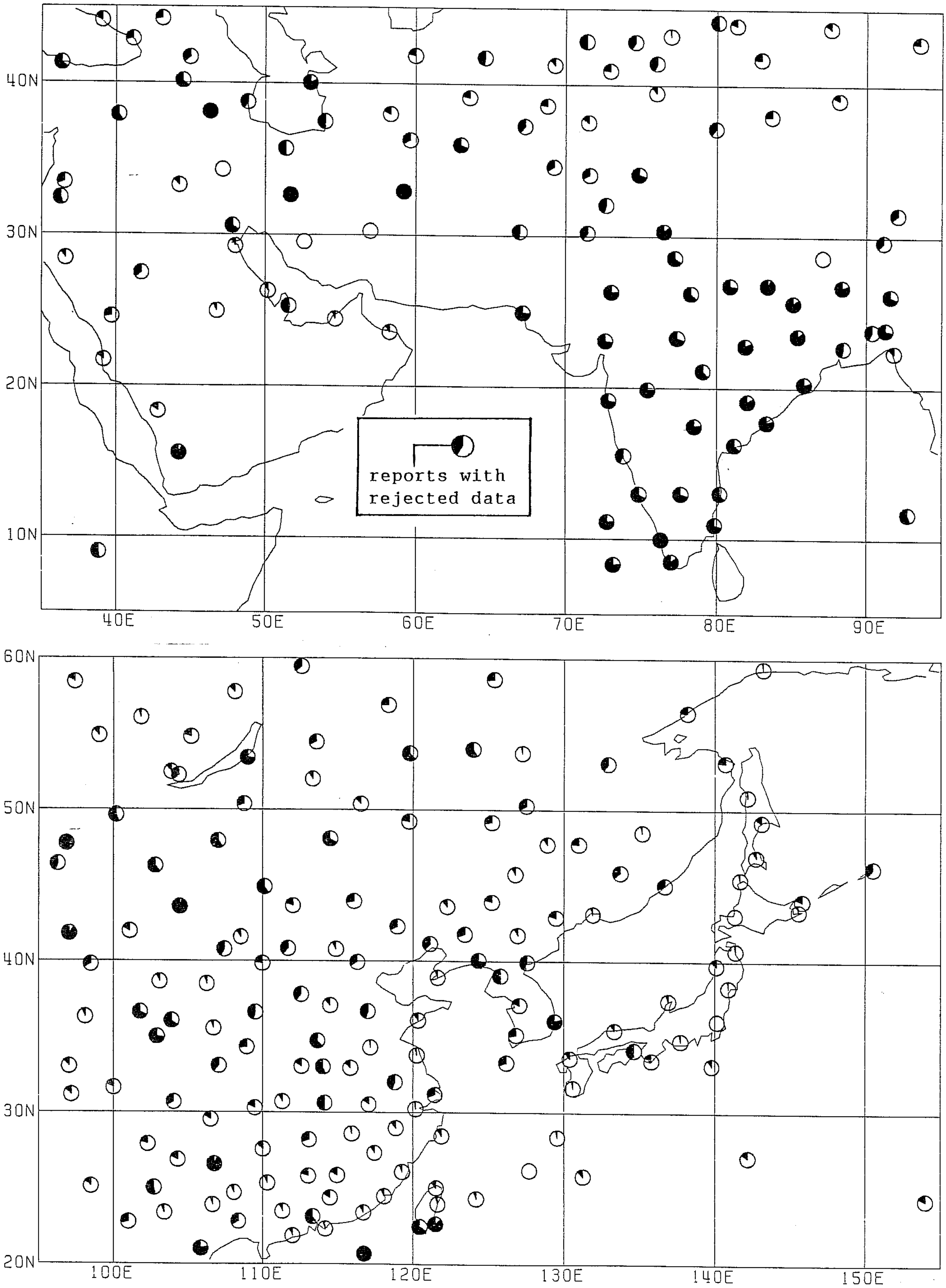

Fig. 4 Ratio of reports with rejected data to all the received reports for TEMP and PILOT Part-A in December 1988. Black sector indicates reports with rejected data.

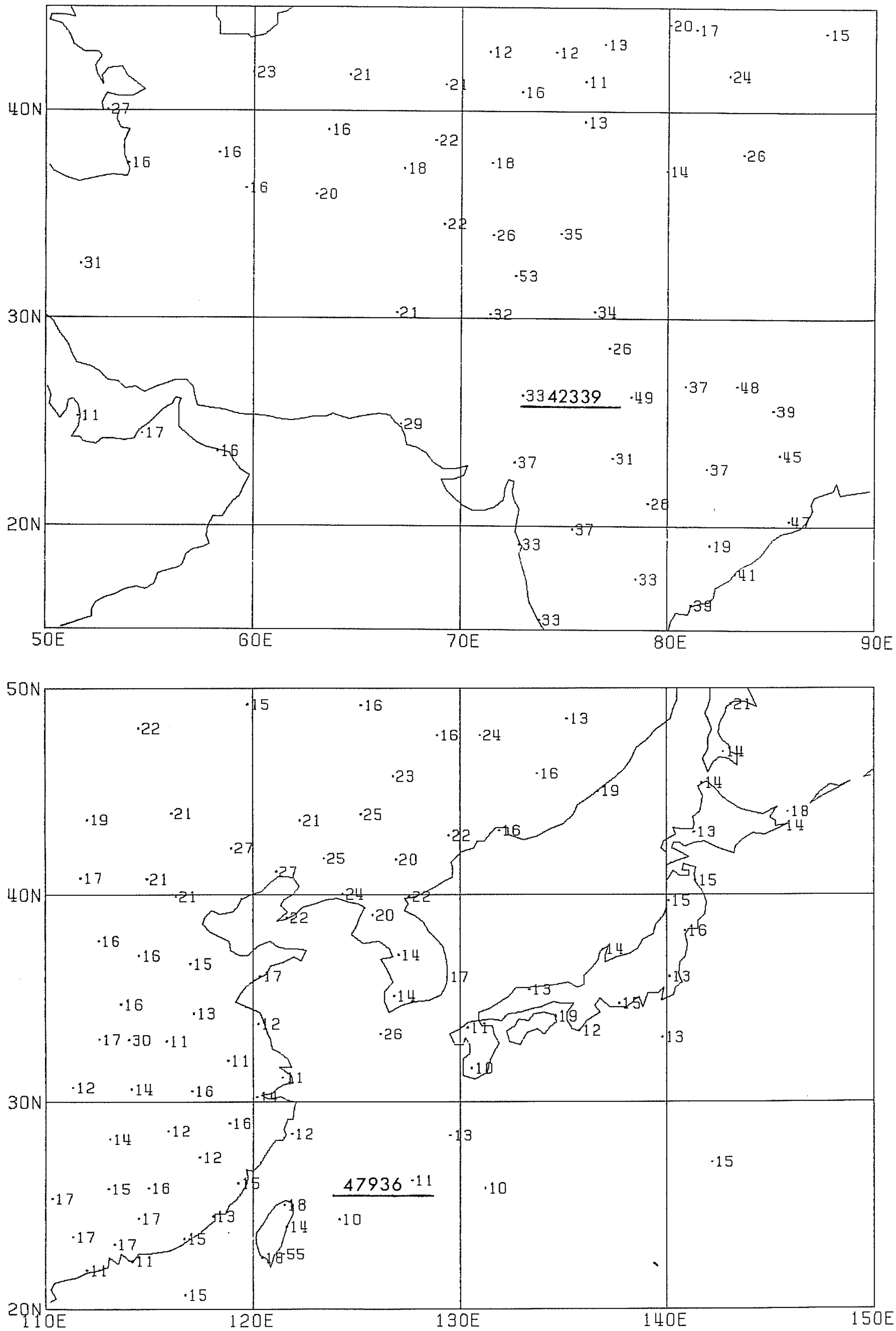

Fig. 5 Root mean square geopotential height difference between observations and first-guess at 500hPa for December 1988, 00 and 12 UTC data. (Units : m)

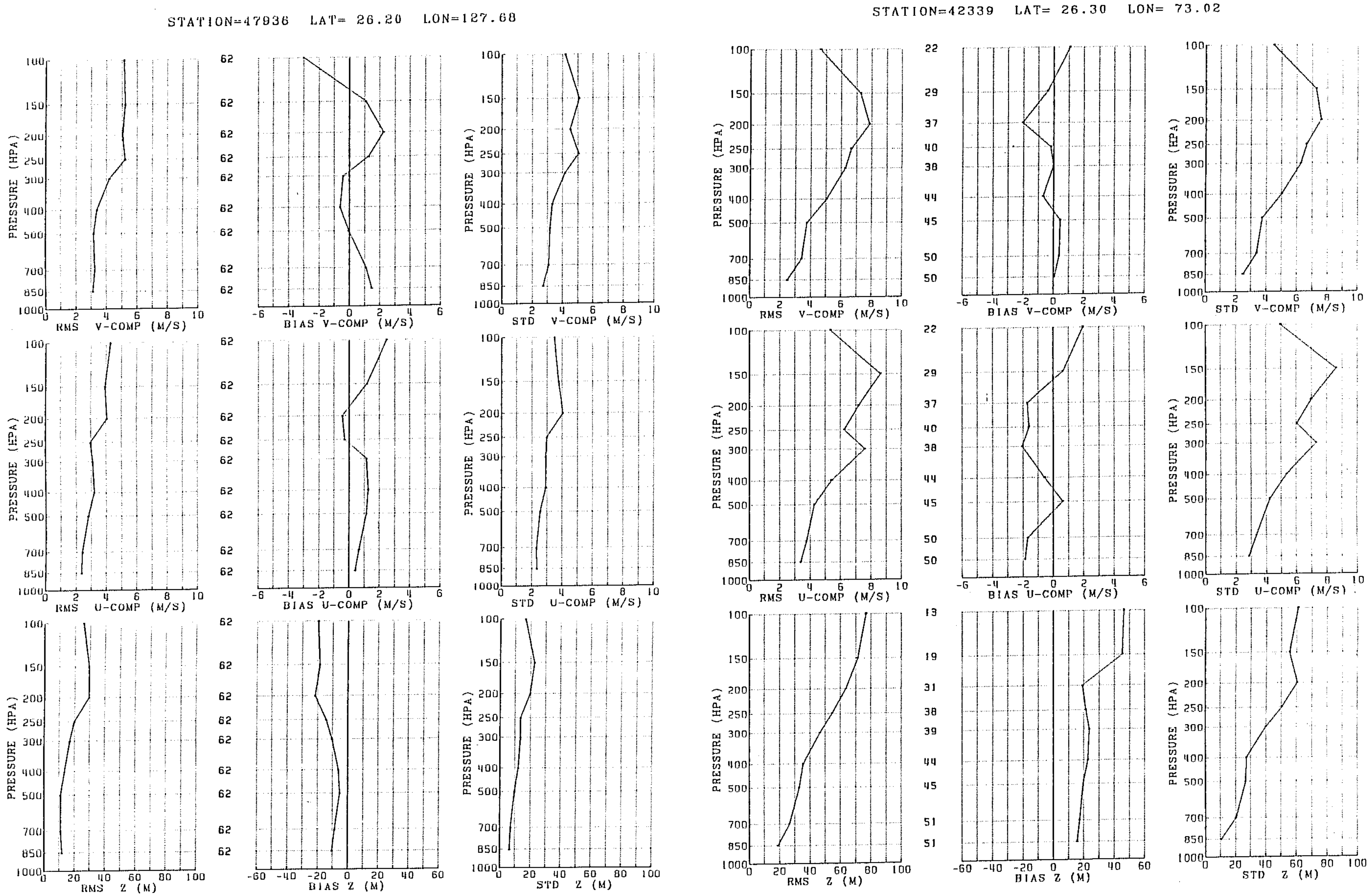

Fig. 6 Vertical profiles of monthly statistics on first-guess minus observation differences at 47936 and 42339 for December 1988, 00 and 12 UTC data.

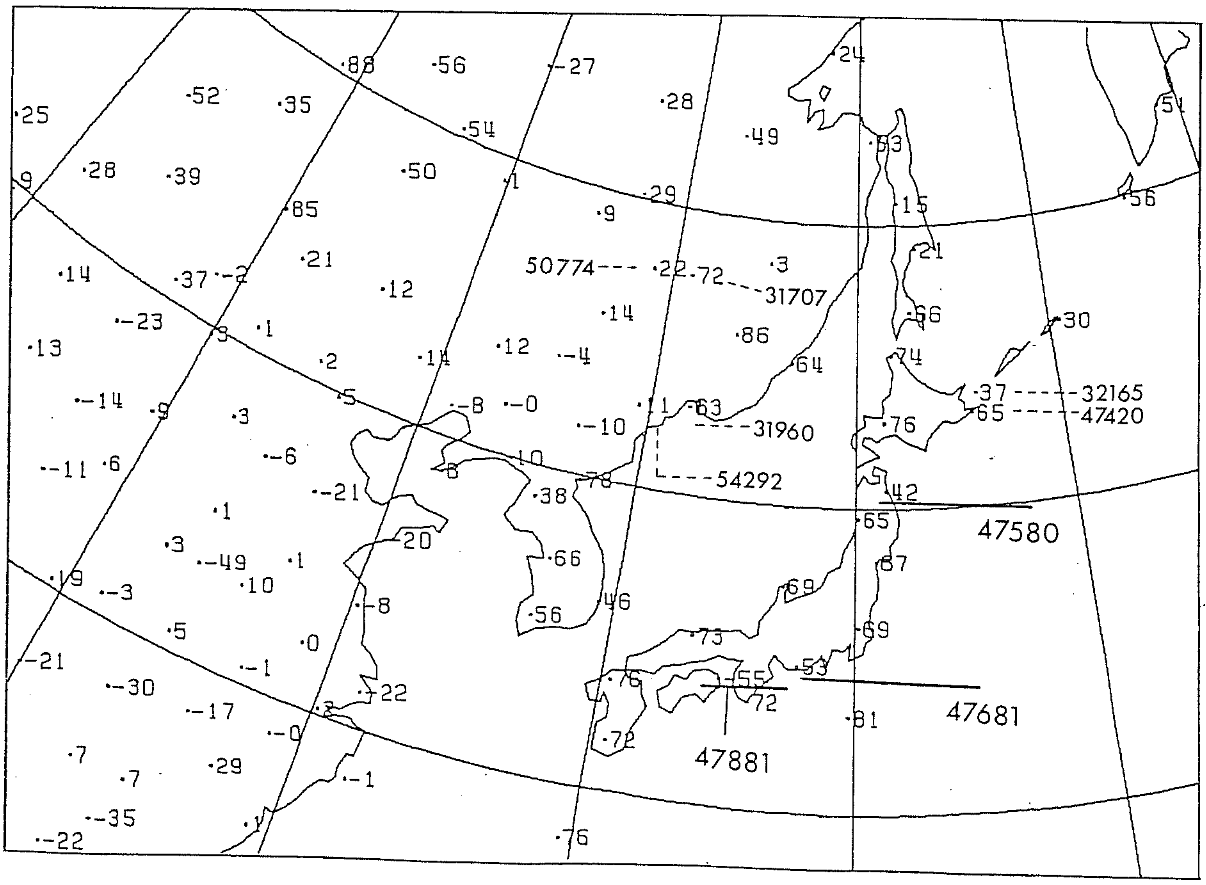

Fig. 7 Mean first-guess minus observation difference of geopotential height at 100hPa for July 1983 00 UTC data. (Units : m)

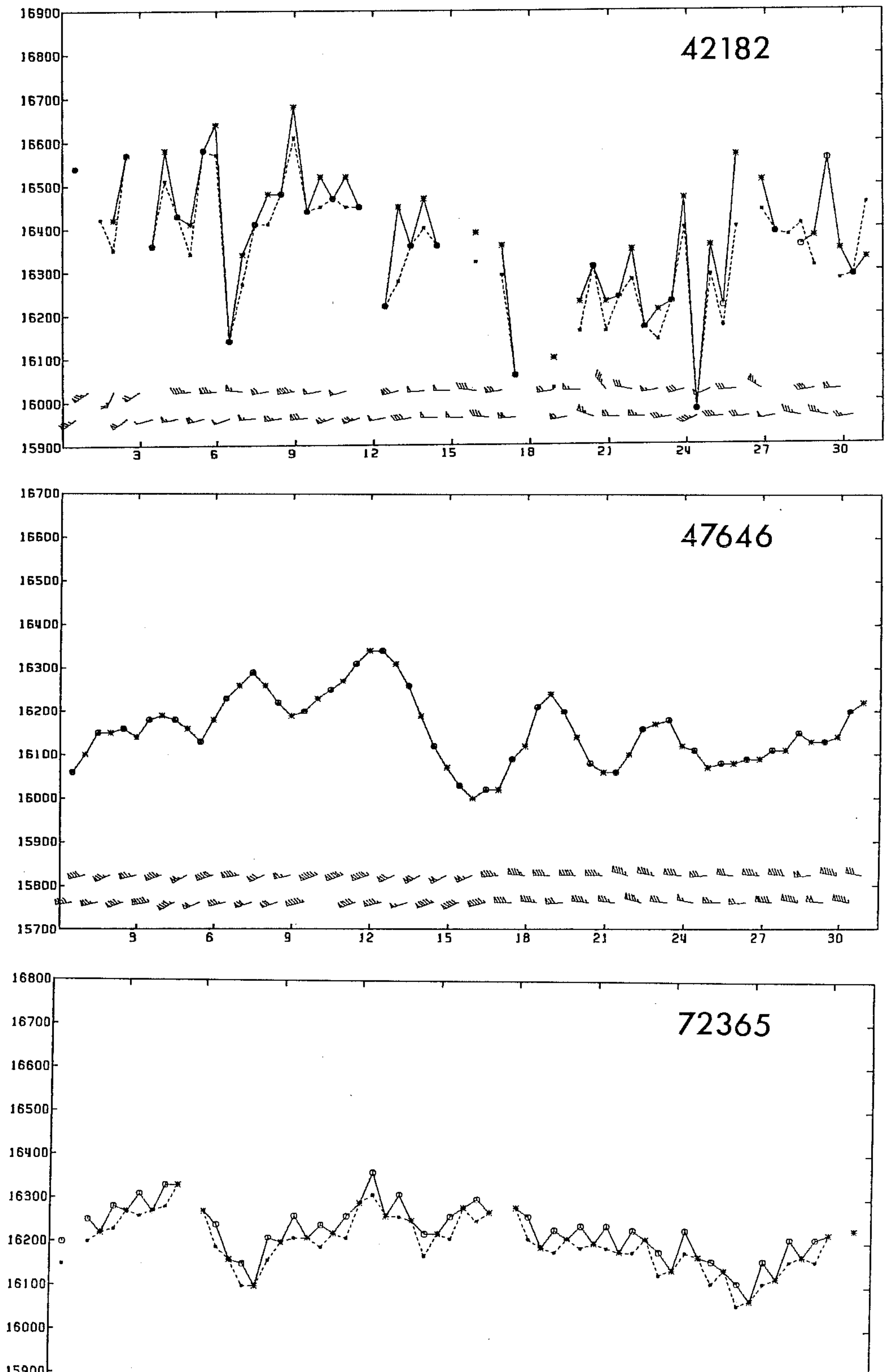

Fig. 8 Time series of 100hPa geopotential height at 42182 (TOP), 47646 (middle) and 72365 (bottom) during December 1988.

solid line : reported value
broken line : corrected value by JMA statistical method and vertical check

INDEX NUMBER OF STATION	YEAR			
	1985	1986	1987	1988
47401	5	11	5	3
47412	17	12	7	0
47420	10	19	7	6
47582	16	19	17	12
47590	48	27	16	6
47600	7	9	4	4
47646	19	0	0	1
47678	4	18	13	13
47744	4	3	5	3
47778	22	11	8	4
47807	11	11	8	4
47827	18	10	5	7
47909	16	29	12	3
47918	2	2	3	3
47936	4	3	0	0
47945	3	2	1	5
47971	8	10	8	15
47991	21	9	7	11
TOTAL	236	205	126	100

Table 2 Number of data rejected in vertical consistency check during the month of April from 1985 to 1988.

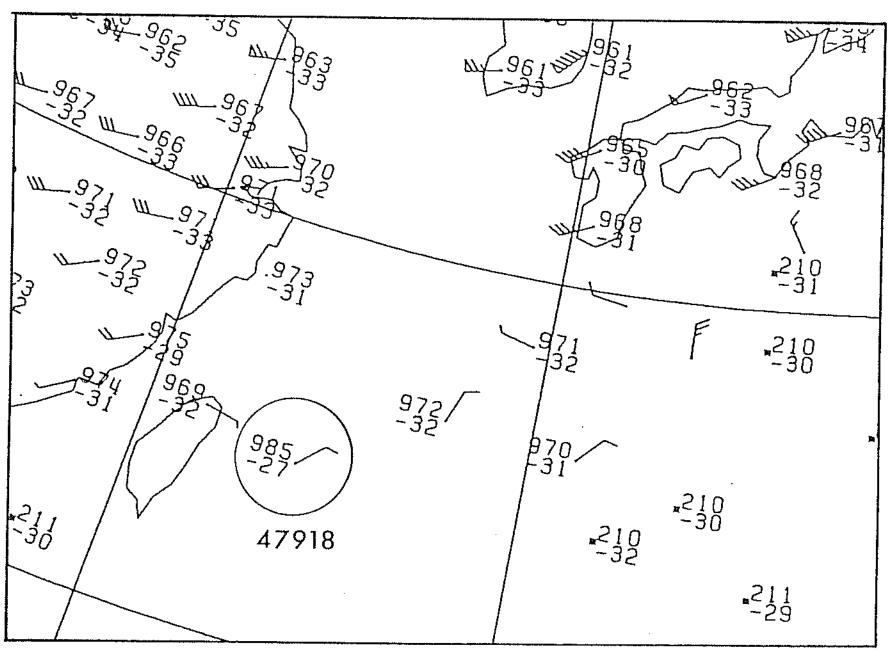

Fig. 9 Observations at 300hPa level, 00 UTC 22 September 1985.

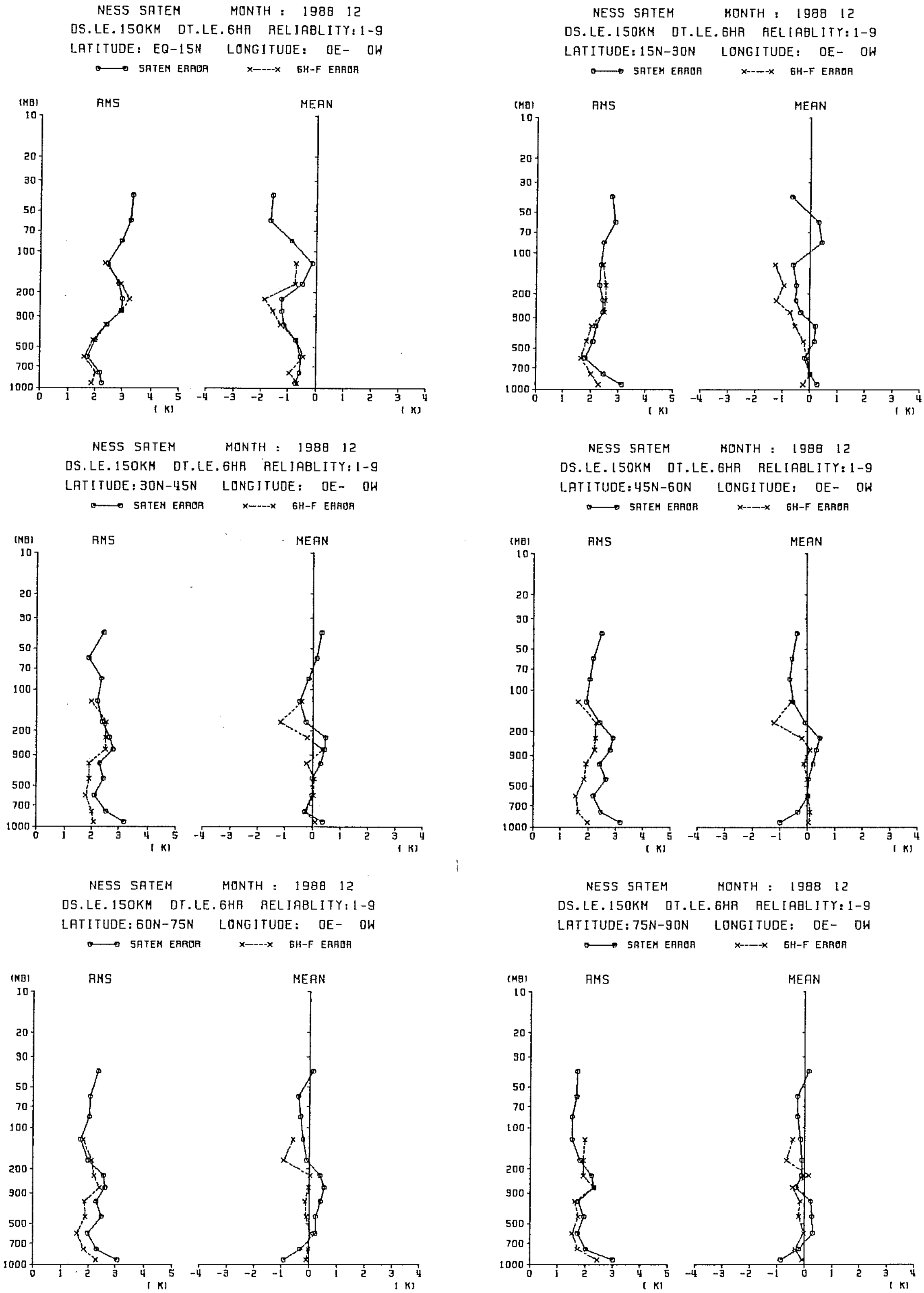

Fig. 10 RMS and mean difference of thickness temperature between sonde data and collocated SATEMs (solid line), and between sonde data and first-guess interpolated at SATEM observation point (broken line).